CHAPTER 1

INTRODUCTION

1.1 Background of Study

After million years of evolutions, insects possess many advanced capabilities and sophisticated mechanisms. Insects were the first organisms on earth to rise into the air. The existence of wings made insects faster and more maneuverable, enabled them to migrate regularly, and greatly complicated their behavior. Developing and designing a Micromechanical Flying Insect (MFI) is the major task for this project. So far the Americans have invested 2.5 million dollars to make this project a success. An important factor in this project is the design of the robofly mechanism which enables the transmission from oscillating piezoelectric actuator to flapping motion. Piezoelectric actuators and flexible thorax structures provide the needed power density and wing stroke to keep the object in the air and solar cells can supply the required source of power

The high acceleration rates and short reaction times make piezoelectric elements suitable towards the mechanical shaking excitation for test purposes within microseconds range. This characteristic of piezoelectric technology has been made useful especially in robot insect technology. The vibrating nature of the piezoelectric material can be used to create a flapping robot insect by their natural resonance.

1.2 Problem Statement

Robofly or Fly robot is a flying robot which mimics the real insects, flies to function. There will be many useful future applications of such an insect robots. Currently, there have been several mechanisms to drive the flapping of wing of such a robot. One of the possible mechanisms is based on periodic deformation of piezoelectric ceramic crystals under oscillating input voltages from an oscillator. The possible design employing the use of piezoelectric crystal need to be explored both on paper and implemented physically.

1.3 Problem Identification

Basically, the problem in this project is to relate the deflection amount of a certain piezoelectric length to the maximum angle for the wing to flap. From the research, it has been identified that the robofly will be able to take off provided the angle of flapping is 120 degrees.

 Second problem is the frequency of the piezoelectric actuator since the flapping rate of the wing directly depends on the actuator. Constant current flow through the piezoelectric ceramic has to be monitored so that the wing will flap at constant frequency to give constant velocity for the robofly.

1.4 Significance of Project

The significance of this project is that in the future, other companies which have the interest to develop a robofly based MFI would refer to this project as a benchmark before doing experimental tests. Companies as well as universities can improvise what have been achieved in this project to commercialize the usage of micromechanical flying insect. There will be a lot to improve in terms of the aerodynamics, lifting forces, materials of the robofly, and the design improvement for the thorax.

1.5 Project Objectives

a) To design and implement the usage of a robofly technology which is tiny, maneuverable, and cost saving.
b) To design and implement a working model/prototype of a possible mechanism for the flapping of wings of fly robot actuated by using piezoelectric crystals.
c) Integrate the working principle of a piezoelectric crystal and transform to wing flapping motion.

1.6 Scope of Study

This project applies both mechanical and electrical engineering principles in order to generate such robot. The scope is narrowed to the design of the flapping mechanism related to kinematics and dynamics principles.

CHAPTER 2
LITERATURE REVIEW

2.1 Micromechanical Flying Insect (MFI)

The design of the MFI is guided by the studies of flying insects. The requirement for a successful fabrication, such as small dimensions, low power consumption, and high flapping frequency are challenging and requires a lot of research. The MFI wings must be capable of independently going through a wing stroke of 120°, while being able to rotate at 90° at a resonant frequency of 150Hz. To achieve this, the body of the MFI consists of 2 wings, each driven by separate thorax structures.

The MFI is designed based on biomimetic principles to capture some of the exceptional flight performance achieved by true flies. The high performance of true flies is based on large forces generated by non-steady state aerodynamics, a high power-to-weight ratio motor system, and a high-speed control system with tightly integrated visual and inertial sensors. Piezoelectric actuators and flexible thorax structures can provide the needed power density and wing stroke, and that adequate power can be supplied by lithium batteries charged by solar cells. (Source taken from Biometic Milisystem Lab website)

The fabrication of such inch-size microrobot requires the design of several components such as thorax design, power supply and also the control system unit. Development in the thorax design will lead to the motion of the wing and also the dynamic of the robofly itself.

Figure 1 shows a Micromechanical Flying Insect (MFI) picture where the robot rests on a tripod of solar panels and has polyester wings and stainless steel struts. The wings aren't able to do the complex arcs that a fly can manage, but they can do simple things, like flap and rotate.
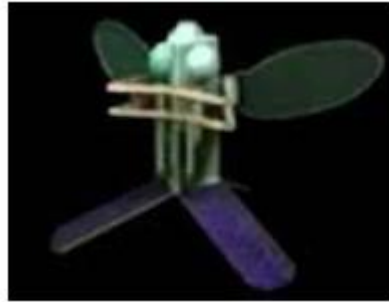
Figure 1: MFI sample (Source from Microrobotics Using Composite)

The MFI consists of several parts, actuators, four-bar structures, airframe, wings, slider crank, power supply, and differential. A differential allows the wing to move in the rotational direction which gives the feathering ability to the MFI. In this particular project, the differential part was not being taken into consideration since the scope of this project mainly focusing on the flapping mechanism.
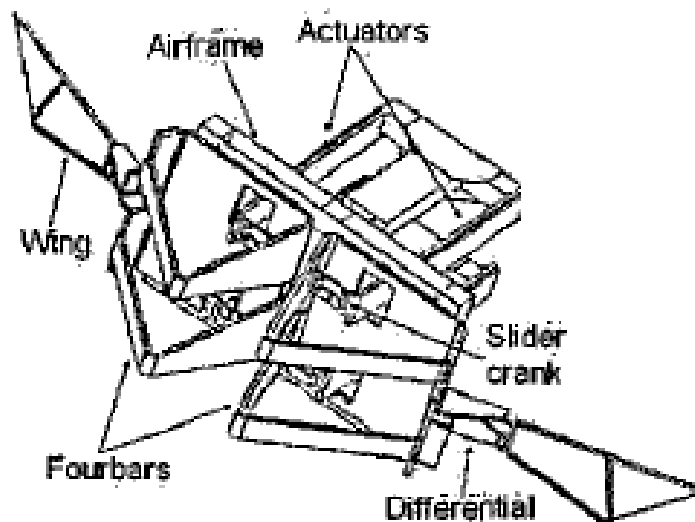
Figure 2: 2 actuators, 2 wing MFI (Source from Microrobotics Using Composite)

2.2 Piezoelectric Ceramic as an Actuator

When a piezoelectric ceramic element is stressed electrically by a voltage, its dimensions change. When it is stressed mechanically by a force, it generates an electric charge. If the electrodes are not short-circuited, a voltage associated with the charge appears. Piezoelectric crystals are widely used in smart structure applications due to their high bandwidth, high output force, compact size, and high power density properties. For such reasons they are very appealing for mobile microrobotic applications such as the Micromechanical Flying Insect.

Relationships between applied forces and the resultant responses depend upon:
- Piezoelectric properties of the ceramic
- Size and shape of the piezoceramic piece
- Direction of the electrical and mechanical excitation.

Piezoelectric ceramics are ferroelectric materials. Above a certain temperature (Curie temperature) the crystal have a centre of symmetry and therefore no electric dipole moment. Elementary cell is cubic where 3 crystal axes have the same lengths and a positively charged Ti/Zr ion is centered on the lattice. The crystal structure undergoes a phase change into the ferroelectric state where the structure is not symmetric. The behavior of the PZT elementary cell is described in **Figure 3.**
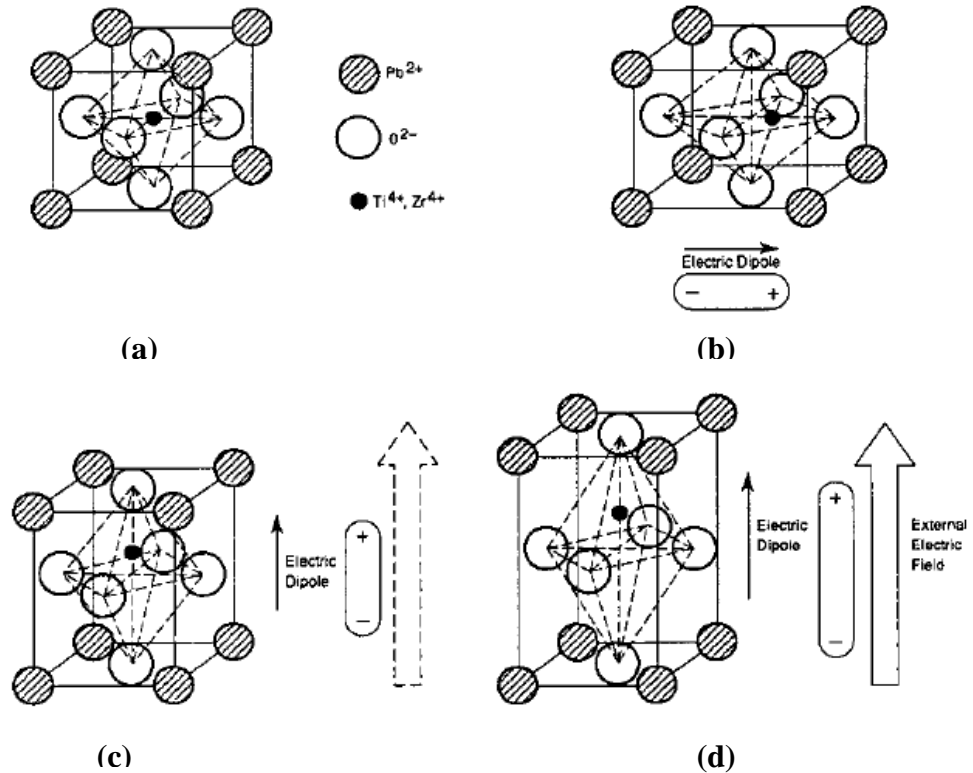
Figure 3: (a) The elementary cell above the Curie temperature; no electric dipole, **(b)** Elementary cell below Curie temperature; generation of the electric dipole, **(c)** turning of the electric dipole using external electrical field, **(d)** elongation of the elementary cell by an external electric field. (Source from Piezoelectric Actuators, Marek Novotny, Pekka Ronkanen)

From macroscopic view, piezoelectric ceramics consist of many such domains, forming large dipole moments. The domains are scattered randomly, hence the net external electric dipole is zero. When the piezoelectric is subjected to a large electric field, the domain dipoles align in the direction closest to the field. Each domain is permitted to several allowed directions which makes a reasonable degree of alignment can be achieved, and makes the material elongated in the same direction. The material remains partially polarized even when the voltage is removed. The material has become permanently piezoelectric and can convert electrical energy to mechanical energy and vice versa, due to the poling as illustrated in **Figure 4**.
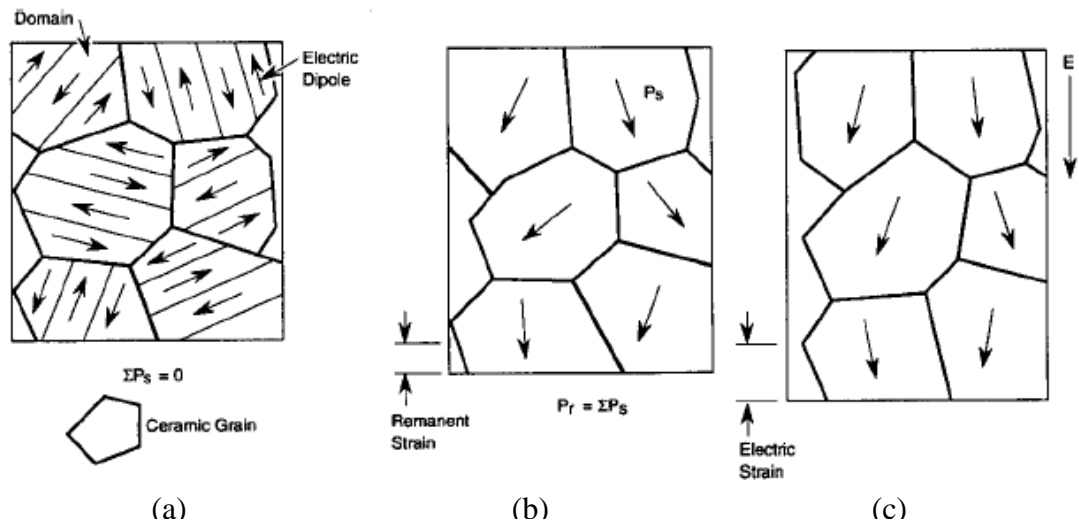
Figure 4: Behavior of piezoceramic material. (a) Non-polarized state, (b) polarized state, (c) electric applied after poling. (Source from Piezoelectric Actuators, Marek Novotny, Pekka Ronkanen)

Piezoelectric actuators can be generally characterized by the piezoelectric coefficients that they exploit (namely d33, d31, and d15). For example:

- a 33-mode piezoelectric actuator produces displacement in the same direction as an electric field applied parallel to the material's polarization direction.

- a 31-mode piezoelectric actuator produces displacement perpendicular to an electric field applied parallel to the material's polarization direction. Approximately twice the strain can be obtained from a 33-mode piezoelectric actuator than a 31-mode piezoelectric actuator for the same applied field; this is due to the relative magnitudes of the piezoelectric coefficients.

- a 15-mode piezoelectric actuator exploits the shear strain produced by an electric field applied perpendicular to the material's polarization direction. Shear strain piezoelectric actuators are not as popular as other piezoelectric actuators since they are difficult to manufacture.

For this project, a standard rectangular shape unimorph actuator (d31 mode) under activation is illustrated in **Figure 5**. The actuator consists of a single piezoelectric layer bonded to a purely elastic layer, usually aluminums, steel or titanium. To maximize the weight of the robofly, aluminium is the best choice for the elastic layer since it has very good elastic characteristic and very light. When a voltage is applied across the thickness of the piezoelectric layer, longitudinal and transverse strain develops. The elastic layer opposes the transverse strain which leads to a bending deformation.
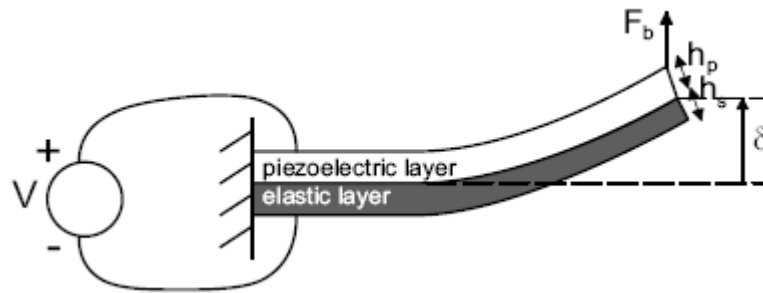
Figure 5: Basic cantilevered rectangular shape unimorph actuator structure. (Source taken from Development of PZT and PZT Based Unimorph Actuators for MFI, University of California)

For a free deflecting unimorph actuator, tip displacement δdc, blocking force Fb, resonant frequency *f*r, mechanical stiffness Km, and mechanical quality factor Qa are defined as below:

Tip displacement, **δdc** $= \dfrac{3\ell^2}{h_p^{\,2}} \dfrac{AB(B+1)}{D} d_{31}V$

Blocking force, **Fb** $= \dfrac{3wh_p}{4s_p\ell} \dfrac{AB(B+1)}{AB+1} d_{31}V$

Mechanical stiffness, **Km** $= \dfrac{F_b}{\delta_{dc}} = \dfrac{wh_p^{\,3}}{4s_p\ell^3} \dfrac{D}{AB+1}$

Where,

ℓ = Unimorph length

w = Unimorph width

V = Applied voltage

s_s, s_p = Elastic compliances of steel and piezoelectric

h_s, h_p = Thickness of steel and piezoelectric layer

E_s, E_p = Young Moduli of steel and piezoelectric

ρ_s, ρ_p = Densities of steel and piezoelectric

A = $s_p / s_s = E_s / E_p$

B = h_s / h_p

C = ρ_s / ρ_p

D = $A^2 B^4 + 2A(2B + 3B^2 + 2B^3)$

For the PZT-5H, PZT-PT and steel layers, Young Modulus E, density ρ, d_{31},
coupling factor k_{31}, relative dielectric constant $K_3^T = \varepsilon / \varepsilon_0$, and maximum electric
field E_3 values are taken from table below:

Table 1: PZT-5H, PZN-PT, and Steel properties

	PZT-5H	**PZN-PT**	**Steel**
E (GPa)	61	15	193
P (kg/m³)	7500	8000	7872
d_{31} (C/N)	320 x 10^{-12}	950 x 10^{-12}	-
k_{31}	0.44	0.5	-
K_3^T	3800	5000	-
E_3 (V/m)	1.5 x 10^6	10 x 10^6	-

2.3 Thorax Construction

The thorax structure consists of two actuators and two mechanically amplifying four-bar structures for each wing. Since the work done on the air is proportional to the velocity of wing squared, the most important requirements are a high resonant frequency and a large stroke angle.

The robofly actuator drives a four-bar linkage structure consists of hollow beams as links and polymer flexures as joints. There is a slider crank mechanism between the actuator and four-bar which converts the approximately linear motion of the tip from the actuator to a rotation at the base of the four-bar. To make the linkage lighter, the beams should not be in solid structures or in other words by using a honeycomb configuration.

The four-bar structures basically consists of 2 beams and a differential. But in this project, I have the most concern on the flapping mechanism (1 Degree of freedom); hence the differential is going to be replaced with a short beam where the wing will be fixed to.

2.4 Wings

Wings are one of the important parts in MFI construction where by looking at the insect body dynamics perspective, the inertial forces from wings can be neglected. In fact, insect's flapping wings is similar to a helicopter dynamics principle. In order to keep the control inputs smooth and bounded proper wing motions need to be designed to ensure continuity at the end of wingbeats, while still preserving maneuverability during each wingbeat.

Four degrees of freedom in each wing are used to achieve flight in nature: flapping, lagging, feathering, and spanning. This requires a universal joint similar the shoulder in a human. Flapping is an angular movement about an axis in the direction of flight. Lagging is an angular movement about a vertical axis which effectively moves the wing forward and backward parallel to the vehicle body. Feathering is an angular movement about an axis in the center of the wing which tilts the wing to change its angle of attack. Spanning is an expanding and contracting of the wingspan. These are the criterions which enables an insect to fly.

The wings, about half an inch long, 1/20 the thickness of a sheet of paper and made of lightweight polyester, look like miniature paddles, and give the fly a wingspan of about one inch. These wing motions are delayed stall, which enables beating wings to have a high angle of attack and high lift at the same time, wing rotation at the bottom and top of the stroke, which, like the backspin on a baseball, gives more lift; and wake capture, whereby a wing gets extra lift by swishing back through air it set in motion on the previous stroke.

2.5 Airframe Design

Airframe is just simply the body structure of the MFI itself. In order to design the airframe, factors such as weight, size, and material stiffness should be taken into considerations. Because of lift power limitations, the mass of the airframe have to be constrained to the smallest value possible. Airframe need to behave as a rigid body, and thus have the stiffness at least 10 times that of the actuators.

There are 2 main parts on the airframe which consists of the stage and 2 pillars which supports the whole MFI. Stage holds the four-bars on top of it. Theoretical stiffness of the stage can be estimated by taking a cross section at critical locations and calculating the stiffness by assuming that both stage and pillars are single supported cantilevers joined in the center. **Figure 6** below shows the rough drawing of the airframe for MFI.
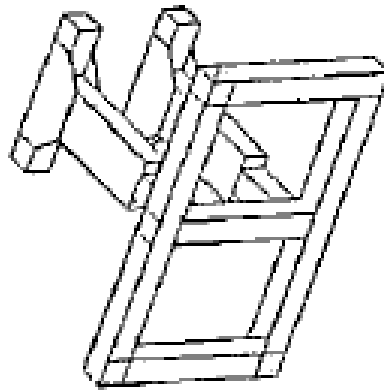
Figure 6: Airframe model by University of California. (Source from Microrobotics Using Composite)

2.6 Power and Control Panel

As applying current from lithium-battery is not reliable for this particular project due to the weight characteristic, the piezoelectric ceramic can be actuated from a natural power source which is from the sunlight. As solar panels having lightweight profile, so it is the most suitable power source for the robofly to take off easily. 3 solar panel which placed at the bottom of the MFI's body will act as legs and at the same time absorbs sunlight to gain energy for the actuator.

There is another type of power source which is currently in development which is the Reciprocating Chemical Muscle (RCM) and normally used in a craft called the Entomopter. Looking more like a giant insect than a scaled down aircraft, the Entomopter has flapping wings and legs and is designed to be used in urban environments. The RCM powered flapping wings and scurrying legs allow the Entomopter to hover and move along the ground. The RCM also produces small amounts of electricity, which can be used to power onboard systems for directional control or other purposes. RCM engines offer a very promising method of powering a MFI, however their development has only recently moved beyond the conceptual phase.

CHAPTER 3

METHODOLOGY / PROJECT WORK

3.1 Methodology Flow Chart

Project work throughout the entire project has been planned during the initiation stage. Based on the project objectives, below is the summary of the project
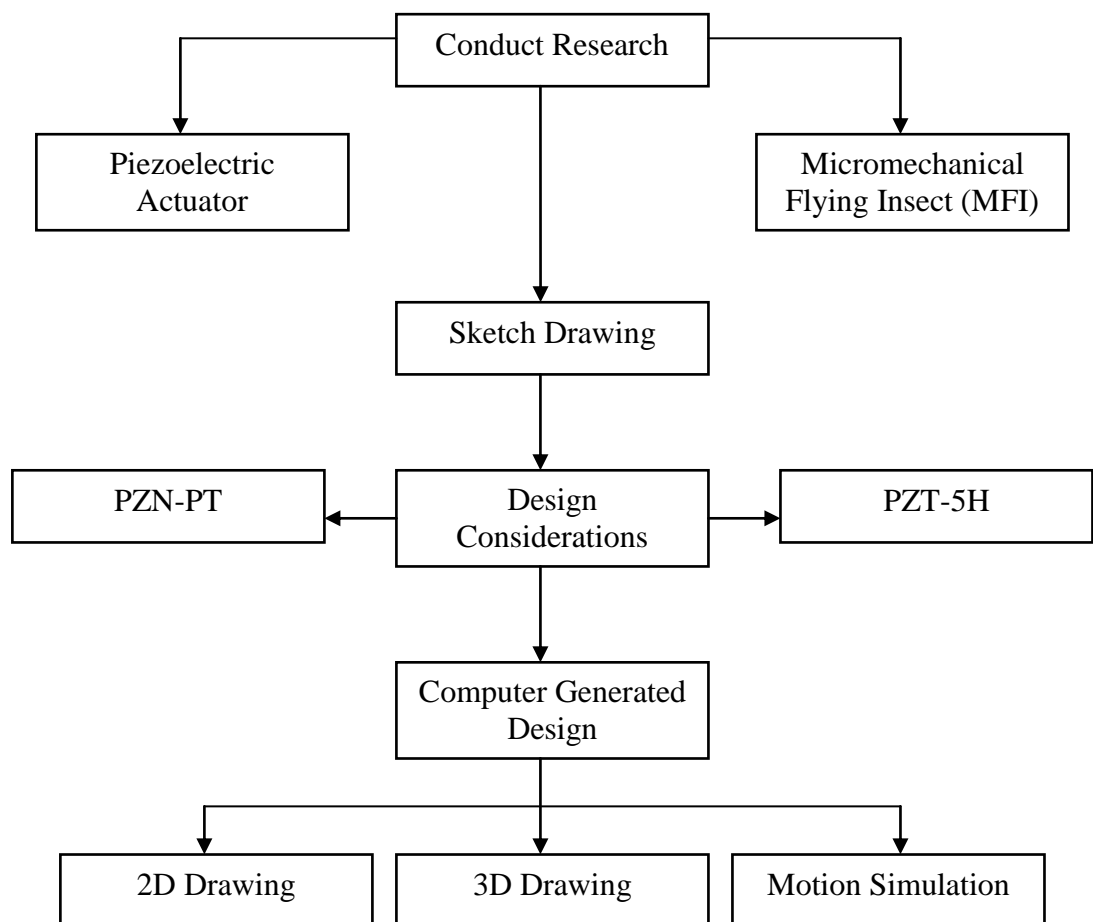

Figure 7: Project work tree

3.2 Research & Study

Research has been conducted and mainly focusing on the mechanism which interacts between the piezoelectric crystal and the wing, where the device eventually capable of sustained autonomous flight. Research being done mainly on the four bar linkage which can convert the deflection of the piezoelectric to flapping motion of the wings. One of the main sources of my research is from the Department of EECS, University of California under the project title 'Microrobotics Using Composite Materials: The Micromechanical Flying Insect Thorax'. It is known that the piezoelectric actuators and flexible thorax structures can provide the needed power density and wing stroke, and that adequate power can be supplied by solar cells.

Learning on design software was also being conducted during FYP1 to familiarize with the simulator design software, ADAMS View. This is powerful software which enables to generate motion analysis and at the same time predict the output of a certain mechanism.

3.3 Tools / Equipments required

The tools and equipment required for this Final Year project is several computer simulated and design software such as AutoCAD, CATIA and ADAMS.

Table 2: Design software tools

Software	Description
AutoCAD 2007	Perform orthographic detailed drawing, with accurate dimension
CATIA V5R12	Generate a 3-dimensional solid model based on the orthographic drawing. Assembly of each part for the model can be performed using this software.
ADAMS VIEW	Perform 2-Dimensional motion simulation and motion analysis.

3.4 Design and Simulation

Sketches and rough drawing will be the kick-off for this process. Several ideas being brought up and analyzed. Design software such as CATIA and ADAMS View were used for the 3D image generation and simulation. The concept of the four-bar linkage is as below.
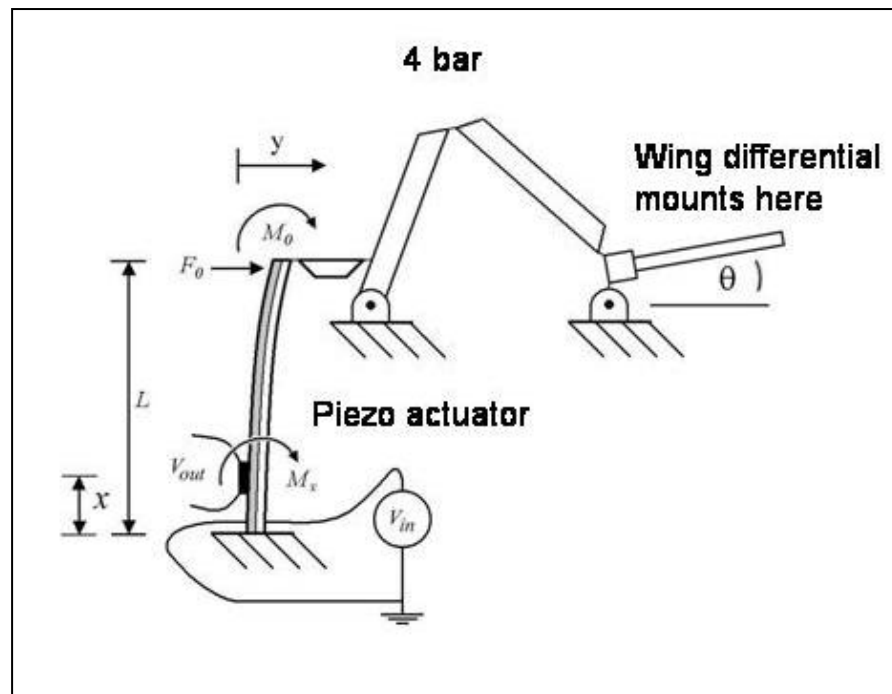
Figure 8: Basic idea of connecting the four-bar, wing, actuator, and input voltages

- V_{in} indicates the voltage input and the circuit will pass by the piezoelectric to create bending effects.
- L is the actual length of the piezoelectric, θ is the wing stroke angle.
- F_o is the force acting in the y-direction from the piezoelectric to the four-bar linkage.
- The wing is mounted at the end of the four-bar (perpendicular to the shortest link) to create flapping motion.

Sketches and rough drawing will be the kick-off for this process. Several ideas were brought up and analyzed. Design software such as CATIA and ADAMS View were used for the 3D image generation and simulation.

Before actually put the robofly in simulation mode, the dimension of each parts and surfaces of the actual robot is to be defined first. An orthographic drawing using AutoCAD will be best used for this purpose. By having the top, front and side views of the robofly, it will be much easier to generate a solid model and 3D simulation.

3.4.1   2D Scale Design

During the first semester, research has been done completely as well as the design of the MFI on rough paper. In order to get the clear view on the physical structures and accurate dimensions of the MFI, an orthographic drawing which consists of front, top, and side view has to be produced. Software of choice, AutoCAD2007 which is the latest design software published by Autodesk company have the complete tools for 2-dimensional and 3-dimensional design.

Below is the orthographic drawing (top, side, and front view) of the MFI.
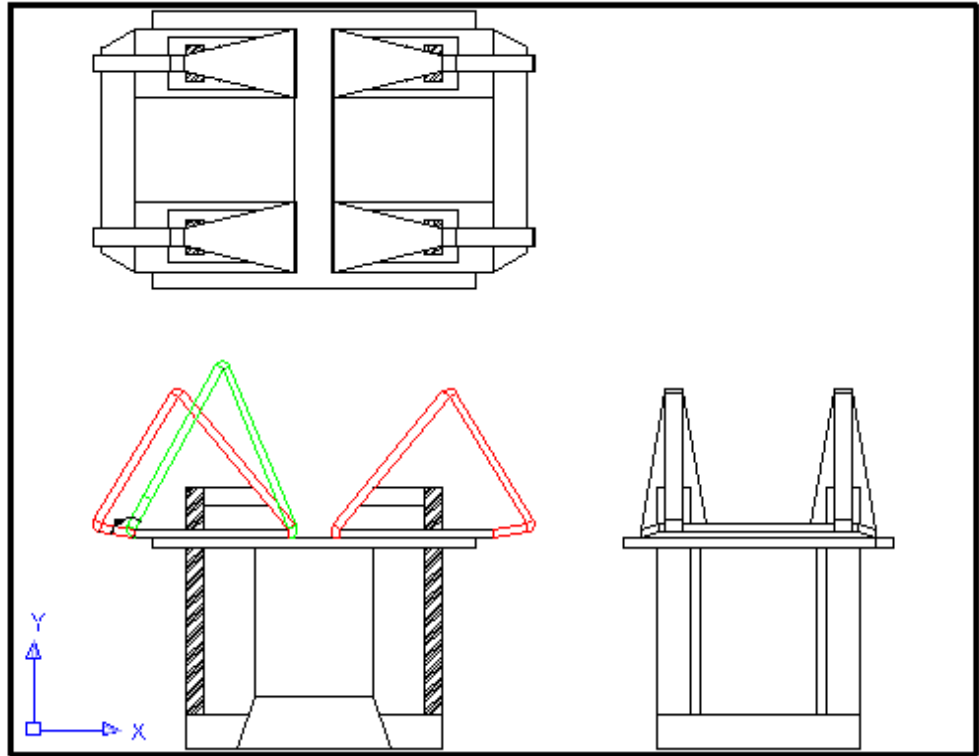
Figure 9: MFI Orthographic drawing

From **Figure 9** above, the hatched areas are representing the piezoelectric and elastic layer. See **Appendix B** for the detail of the dimension of MFI.

3.4.2 3D Modelling / Simulation

In the 3D simulation, the links, joints, and forces have been defined but the simulation is under the state of error for Design 1. Three basic joints used in the simulation; namely fixed joint, rotating joint, and fixed ground rotating joint. In the simulation, the actuator and slider crank is represented by a triangular link where it pushes the longest link of the four-bar and gives an upstroke & downstroke for the wing. Below is the design of the MFI's thorax using ADAMS software.
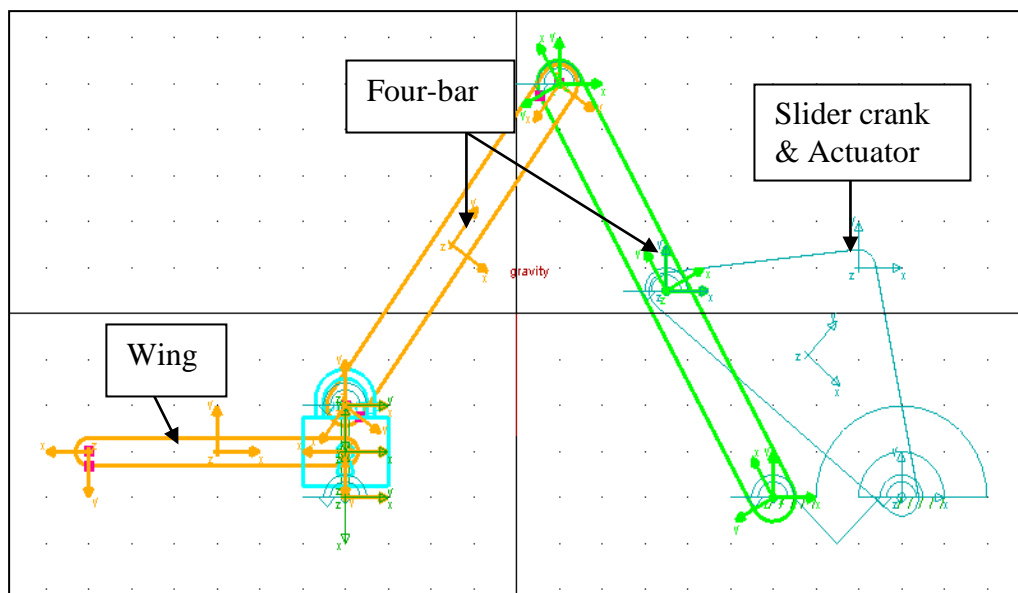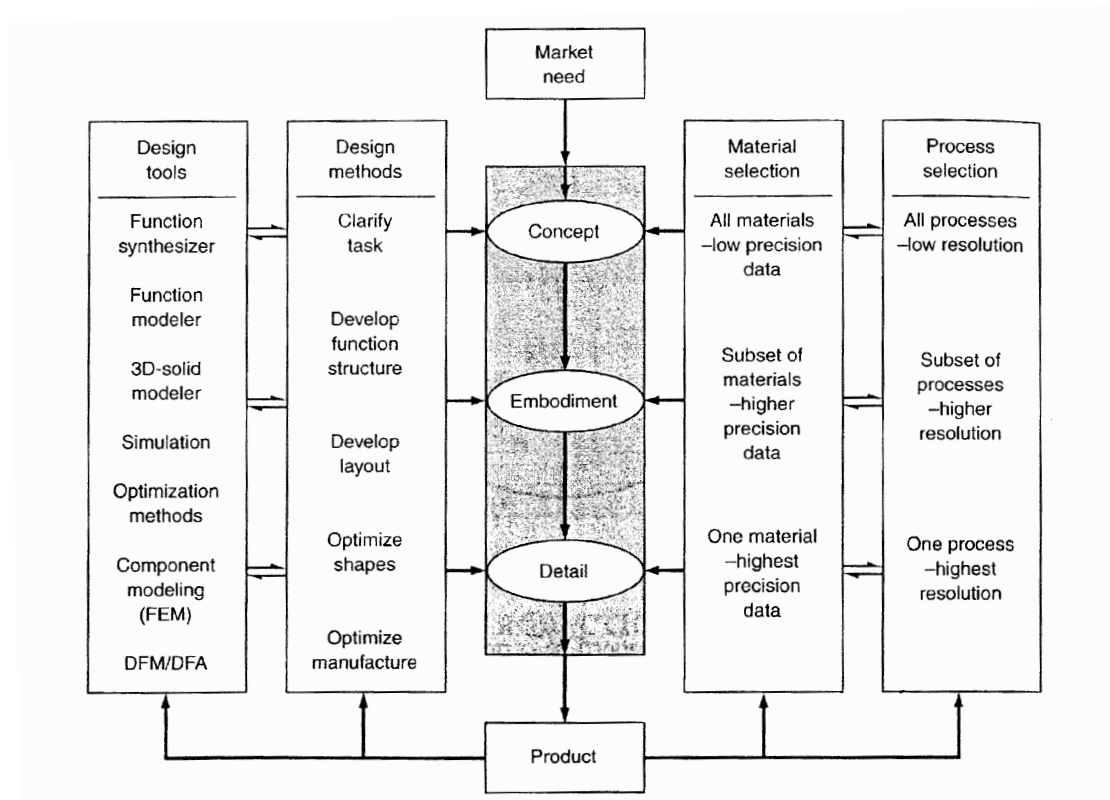

Figure 10: 3D MFI thorax simulation set-up

See **Appendix A** for different view of the design.

3.5 Design Process Tools

Figure 11: Table for Schematic of Design Process

This table guides me to narrowing down the process used to achieve the best combination of material and manufacturing process. It also acts as a guideline for this project and covers every aspect throughout the success of this project. Under the design tools, I have determined the function synthesizer about the robofly where the actuator, thorax, wing, and power supply works as one system. Then, I focused more on each function separately in details previously (in the literature review section).

CHAPTER 4
RESULTS AND DISCUSSION

4.1 Actuator Design Considerations

Taking the microaerial flapping mechanisms as the target application, design issues, selection of proper actuator, and its characterization are investigated. PZN-PT and PZT-5H are investigated as the possible piezoelectric layers as suggested by Piezo Systems, Inc. for micromechanical flying insect development. The thickness and dimension for both piezoelectric materials proposed are the same. Refer to **Appendix C** for the actuator dimension.

Considering a standard rectangular shape of piezoelectric unimorph actuator, some calculations have been derived for a single piezoelectric layer bonded to a purely elastic layer (steel). Steel was chosen because of its high Young Modulus value, which can sustain the deformation caused by piezoelectric layer.

As discussed in Section 2.2, a free deflecting unimorph actuator are taken into consideration to determine the tip displacement, δ_{dc}, blocking force, **Fb**, and mechanical stiffness, **Km.** But first, some parameters need to be calculated for ease, namely A,B,C, and D and V_{max}. For the design considerations, equations for the actuator design calculations are converted to the rotational motion of the actuator for simplicity.

4.1.1 PZN-PT

1. Calculate value for A, B, C, D, and V$_{max}$

$$A = s_p / s_s = E_s / E_p$$
$$= (193 / 15)\text{GPa}$$
$$= 12.87$$

$$B = h_s / h_p = (0.00005 / 0.0001)$$
$$= 0.5$$

$$C = \rho_s / \rho_p = (7872 / 8000)$$
$$= 0.984$$

$$D = A^2 B^4 + 2A\ (2B+3B^2+2B^3)$$
$$= \left(12.87^2\right)\!\left(0.5^4\right) + 2(12.87)\!\left[\left(2\times0.5\right)+\left(3\times0.5^2\right)+\left(2\times0.5^3\right)\right]+1$$
$$= 10.352 + 52.48$$
$$= 62.832$$

$$V_{max} = E_3 h_p$$
$$= \left(10\times10^6\right)\times(0.0001)$$
$$= 1000V$$

2. Actuator design calculation

Tip displacement, $\boldsymbol{\delta dc} = \dfrac{3\ell^2}{h_p{}^2} \dfrac{AB(B+1)}{D} d_{31}V$

$$= \dfrac{3(0.01^2)}{0.0001^2} \dfrac{12.87 \times 0.5 \times (0.5+1)}{62.832} (950 \times 10^{-12})(1000)$$

$$= 30000 \left(\dfrac{9.6525}{62.832}\right)(9.5 \times 10^{-7})$$

$$= 4.378 \times 10^{-3} \text{ m}$$

Blocking force, $\boldsymbol{Fb} = \dfrac{3wh_p}{4s_p\ell} \dfrac{AB(B+1)}{AB+1} d_{31}V$

$$= \dfrac{3(0.001)(0.0001)}{4(65 \times 10^{-12})(0.01)} \dfrac{12.87 \times 0.5 \times (0.5+1)}{(12.87 \times 0.5)+1} (950 \times 10^{-12})(1000V)$$

$$= 115384.6 \left(\dfrac{9.6525}{7.435}\right)(9.5 \times 10^{-7}) = 0.141 \text{ N}$$

Mechanical stiffness, $\boldsymbol{Km} = \dfrac{F_b}{\delta_{dc}} = \dfrac{wh_p{}^3}{4s_p\ell^3} \dfrac{D}{AB+1}$

$$= \dfrac{0.141}{4.378 \times 10^{-3}}$$

$$= 32.206 \text{ N/m}$$

3. Rotational equation

Actuator rotation angle, $\theta_{dc} = \dfrac{\delta_{dc}}{\ell} = \dfrac{3\ell}{h_p^2}\dfrac{AB(B+1)}{D}d_{31}V$

$$= \frac{4.378\times10^{-3}}{0.01} = 0.4378$$

Output torque, $\tau_a = F_b\ell = \dfrac{3wh_p}{4s_p}\dfrac{AB(B+1)}{AB+1}d_{31}V$

$$= 0.141\times0.01$$
$$= 1.41\times10^{-3}\ \text{Nm}$$

Rotational stiffness, $K_a = K_m\ell^2 = \dfrac{wh_p^3}{4s_p\ell}\dfrac{D}{AB+1}$

$$= 32.206\times(0.01)^2$$
$$= 3.2206\times10^{-3}\ \text{Nm/rad}$$

4.1.2 PZT-5H

1. Calculate value for A, B, C,D, and V_{max}

$$A = s_p / s_s = E_s / E_p$$
$$= (193 / 61)\text{GPa}$$
$$= 3.164$$

$$B = h_s / h_p = (0.00005 / 0.0001)$$
$$= 0.5$$

$$C = \rho_s / \rho_p = (7872 / 7500)$$
$$= 1.0496$$

$$D = A^2 B^4 + 2A\,(2B + 3B^2 + 2B^3)$$
$$= \left(3.164^2\right)\left(0.5^4\right) + 2(3.164)\left[\left(2 \times 0.5\right) + \left(3 \times 0.5^2\right) + \left(2 \times 0.5^3\right)\right] + 1$$
$$= 0.6257 + 13.656$$
$$= 14.2817$$

$$V_{max} = E_3 h_p$$
$$= \left(1.5 \times 10^6\right) \times \left(0.0001\right)$$
$$= 150V$$

2. Actuator design calculation

Tip displacement, δ_{dc} $= \dfrac{3\ell^2}{h_p^{\,2}} \dfrac{AB(B+1)}{D} d_{31}V$

$$= \frac{3(0.01^2)}{0.0001^2} \frac{3.164 \times 0.5 \times (0.5+1)}{14.2817} (320 \times 10^{-12})(150)$$

$$= 30000(0.1662)(4.8 \times 10^{-8})$$

$$= 2.393 \times 10^{-4} \text{ m}$$

Blocking force, $\mathbf{F_b}$ $= \dfrac{3wh_p}{4s_p\ell} \dfrac{AB(B+1)}{AB+1} d_{31}V$

$$= \frac{3(0.001)(0.0001)}{4(65 \times 10^{-12})(0.01)} \frac{3.164 \times 0.5 \times (0.5+1)}{(3.164 \times 0.5)+1} (320 \times 10^{-12})(150V)$$

$$= 115384.6(0.845)(4.8 \times 10^{-8})$$

$$= 4.68 \times 10^{-3} \text{N}$$

Mechanical stiffness, $\mathbf{Km}$ $= \dfrac{F_b}{\delta_{dc}} = \dfrac{wh_p^{\,3}}{4s_p\ell^3} \dfrac{D}{AB+1}$

$$= \frac{4.68 \times 10^{-3}}{2.393 \times 10^{-4}}$$

$$= 19.557 \text{ N/m}$$

3. Rotational equation

Actuator rotation angle, $\boldsymbol{\theta}\mathbf{dc} = \dfrac{\delta_{dc}}{\ell} = \dfrac{3\ell}{h_p^2}\dfrac{AB(B+1)}{D}d_{31}V$

$$= \frac{2.393\times10^{-4}}{0.01} = 0.02393$$

Output torque, $\boldsymbol{\tau}\mathbf{a} = F_b\ell = \dfrac{3wh_p}{4s_p}\dfrac{AB(B+1)}{AB+1}d_{31}V$

$$= \left(4.68\times10^{-3}\right)\times0.01$$

$$= 4.683\times10^{-5} \text{ Nm}$$

Rotational stiffness, $\mathbf{Ka} = K_m\ell^2 = \dfrac{wh_p^3}{4s_p\ell}\dfrac{D}{AB+1}$

$$= 19.557\times(0.01)^2$$

$$= 1.9557\times10^{-3} \text{ Nm/rad}$$

4.1.3   PZN-PT and PZT-5H comparison and discussion

As calculated in earlier section (Section 4.1.1 and 4.1.2), all the values being tabulated in Table 3 below.

Table 3: Design parameters for PZN-PT and PZT-5H actuator

Parameter	PZN-PT	PZT-5H
Max. applied voltage, V_{max} (V)	1000	150
Tip displacement, δ_{dc} (m)	4.378×10^{-3}	2.393×10^{-4}
Blocking force, $\mathbf{F_b}$ (N)	0.141	4.68×10^{-3}
Mechanical stiffness, $\mathbf{K_m}$ (N/m)	32.206	19.557
Actuator rotation angle, $\mathbf{\theta_{dc}}$	0.4378	0.02393
Output torque, $\mathbf{\tau_a}$ (Nm)	1.41×10^{-3}	4.683×10^{-5}
Rotational stiffness, $\mathbf{K_a}$ (Nm/rad)	3.2206×10^{-3}	1.9557×10^{-3}

From the table, PZN-PT piezoelectric gives higher deflection compared to PZT-5H piezoelectric actuator. Other values for PZN-PT based unimorph have higher blocking force, mechanical stiffness, and other rotational parameters compared to PZT-5H. In addition, the maximum allowable voltage applied on PZN-PT based unimorph is much higher than the other piezoelectric ceramic, PZT-5H actuator.

The selection of piezoelectric as actuator will be based on the input requirement from the design. Tip displacement is the parameter that should be focused on since the linear deflection is the driving mechanism to run the four bar thorax structure, ultimately leads to the flapping motion of the wing. Other parameters calculated were the additional information to describe the actuator properties, when the piezoelectric ceramic is bonded with elastic material.

4.2 Two Dimensional Drawing (Orthographic)

The two dimensional drawing of the MFI was generated with the aid of AutoCAD software. Dimensions of each component were defined on a rough paper before start with the computer generated drawing. In order to get the clear view on the physical structures and accurate dimensions of the MFI, an orthographic drawing which consists of front, top, and side view has to be produced.

The initial design (Design 1) is the first draft of the actual robofly where it consists of 2 wings, 4 piezoelectric actuators, a body frame, and 4 four-bar linkages. The design is able to produce 109° of wing stroke angle, during lifting.

However, the improved design (Design 2) can produce wing stroke angle of 120°, which is identified to be the requirements for lifting purpose based on a real insect wing motion. In addition to that, the improved design secures the four-bar linkages (robofly thorax) by installing it inside the body frame rather that outside the body frame in design 1. Refer to **Appendix D** for 3 dimensional parts and assembly drawing for design 2.
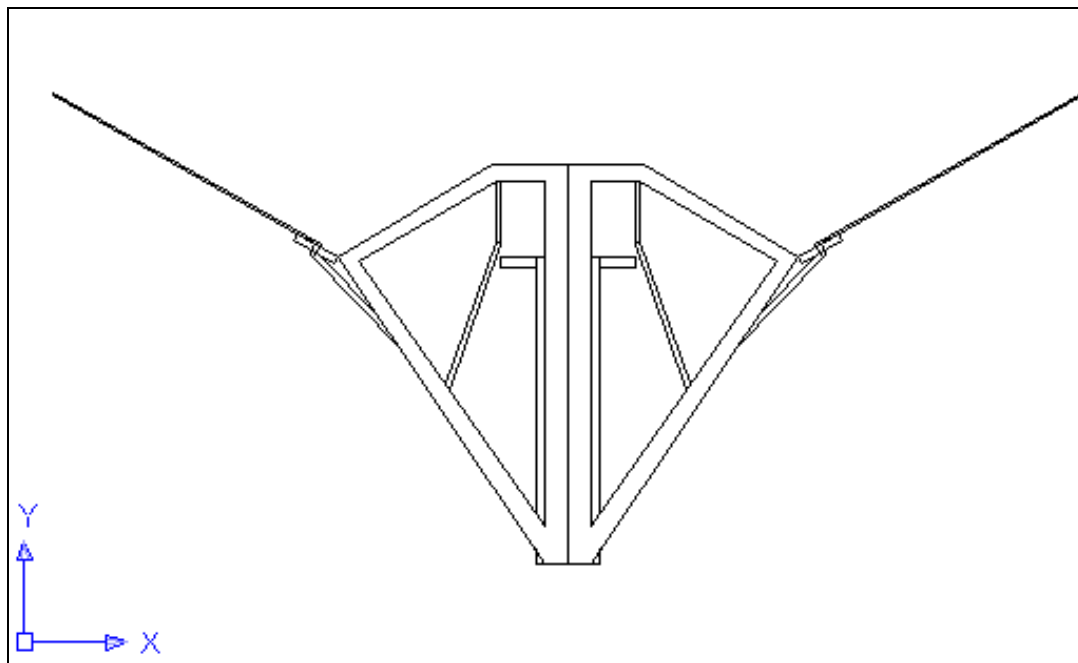
DESENG 1
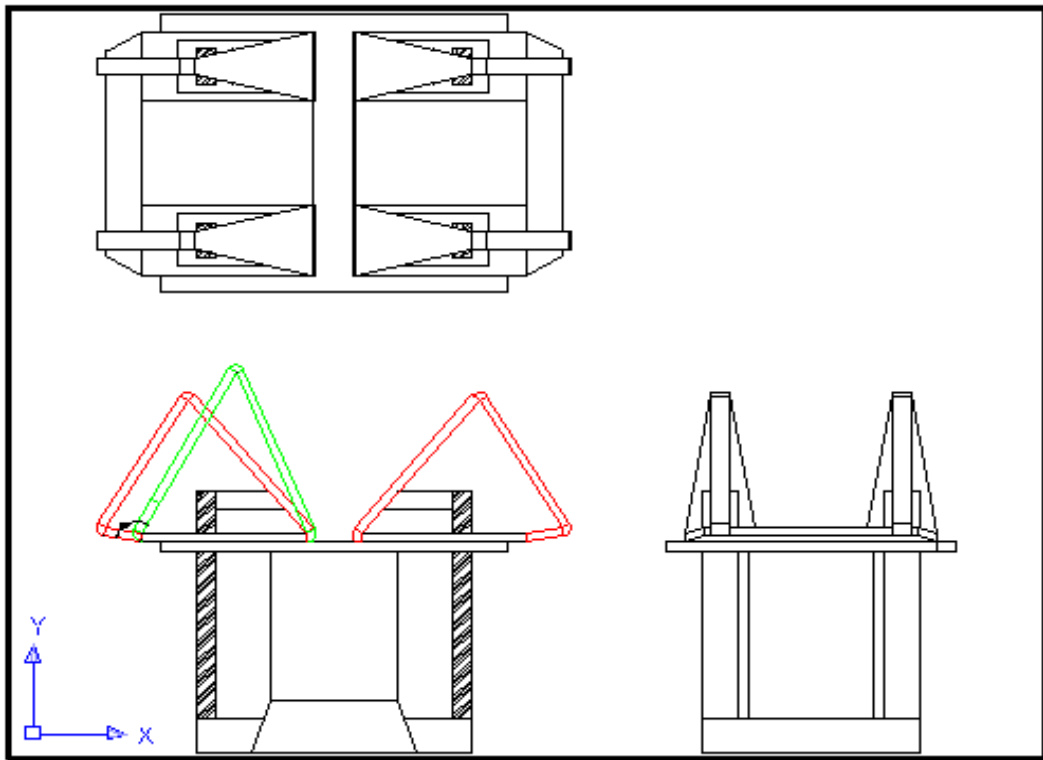
Figure 12: MFI Orthographic drawing (Design 1)

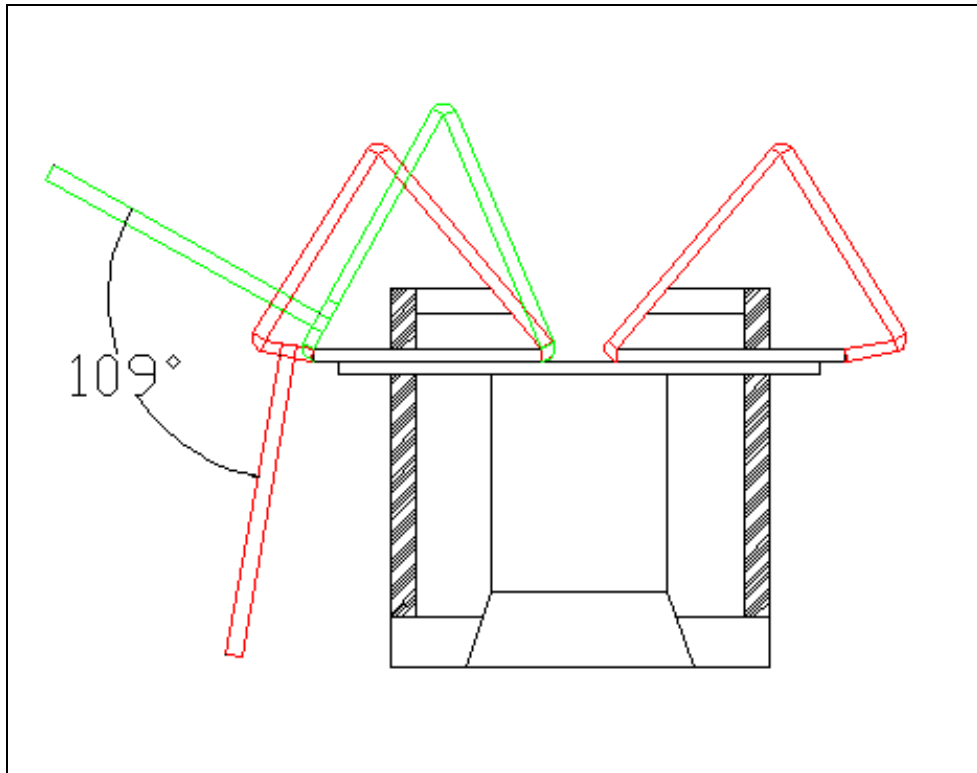**DESIGN 2**
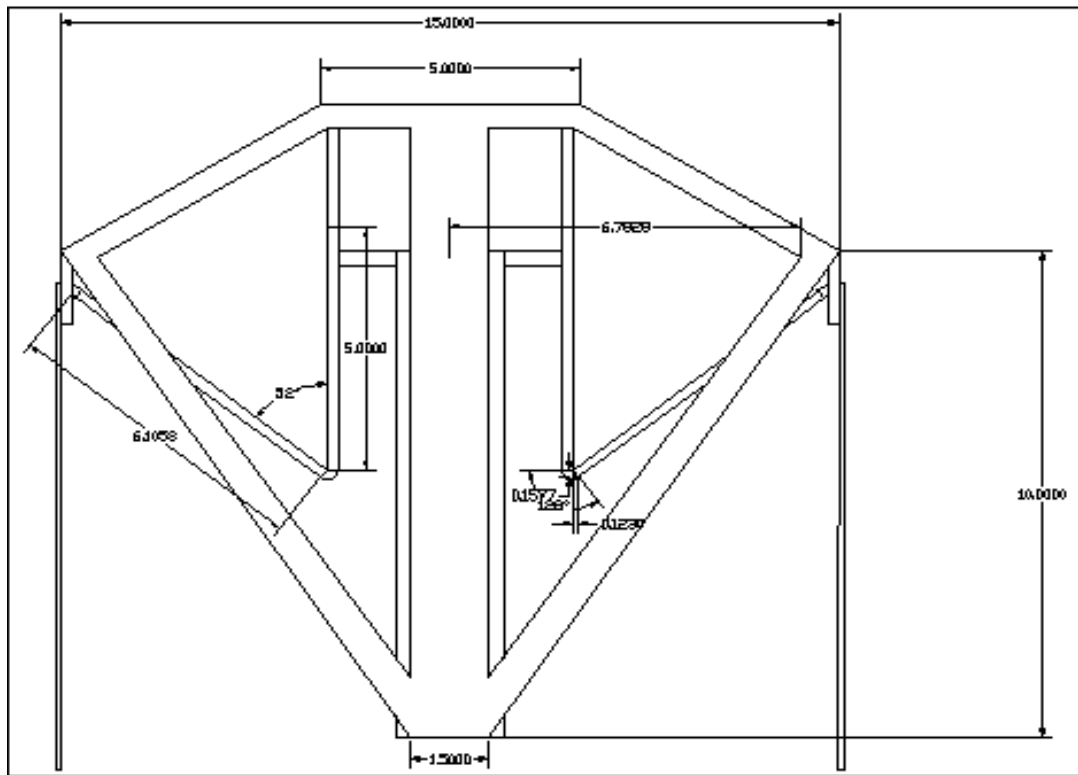
**Figure 13**: MFI Downstroke (Design 2)

Figure 14: MFI Upstroke (Design 2)

4.3 Wing Stroke

In order to get the best lift for the MFI, the difference angle between the upstroke and downstroke should be around 120° (source taken from Microrobotics Using Composite Materials: University of California). The four-bar consists of 3 beams which have its own unique length to provide such output. By using the cosine rule of triangle, **Figure 15** below is the length of the beams which gives 109° of wing stroke angle. However, the improved design in **Figure 16** gives a better wing stroke angle which equal to 120°. The green line indicates the four bar structure during wing upstroke, while the red line indicates the four bar mechanism during wing downstroke.

- For Design 1, the required actuator linear deflection is 0.601mm to produce maximum angle stroke of 109°.
- For Design 2 however, smaller actuator deflection needed to produce better angle stroke of 120°. Linear deflection of 0.166mm is essential for this purpose.

**Figure 15**: Four-bar dimensions and wing stroke angle (Design 1)
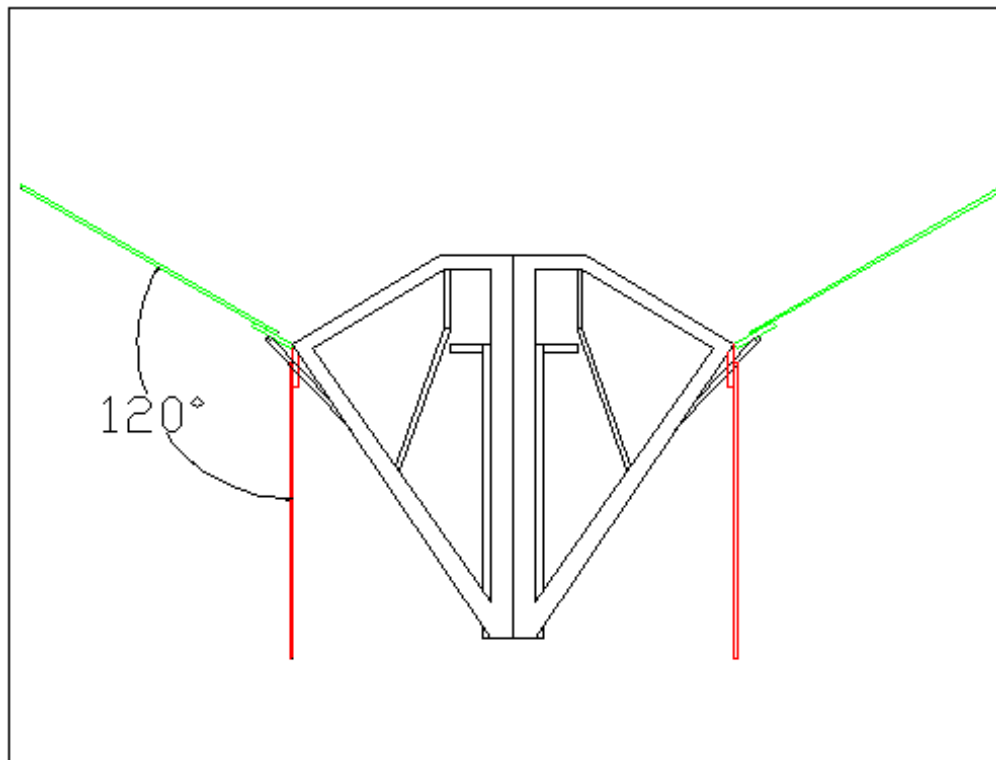
Figure 16: Four-bar dimensions and wing stroke angle (Design 2)

4.4 MFI Simulation

3D simulation for the robofly is applied especially on the actuator, thorax and wing. Using the defined length for all the items stated, a motion simulation is successfully obtained for the robofly wing. From the simulation, it can be observed that the transformation from piezoelectric bending effect to wing flapping motion is achievable.
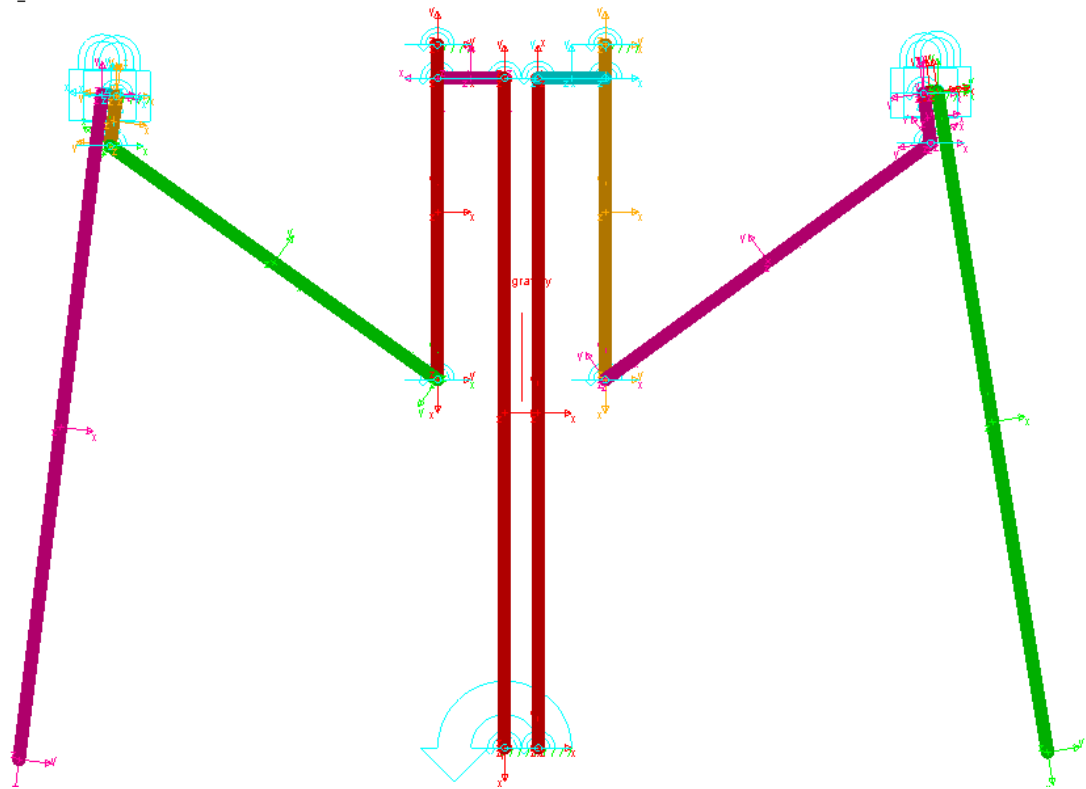
To simplify the simulation for design 1, bending effect from the piezoelectric actuator is represented by a rotating motor acting on the base of the actuator itself.

DESIGN 1
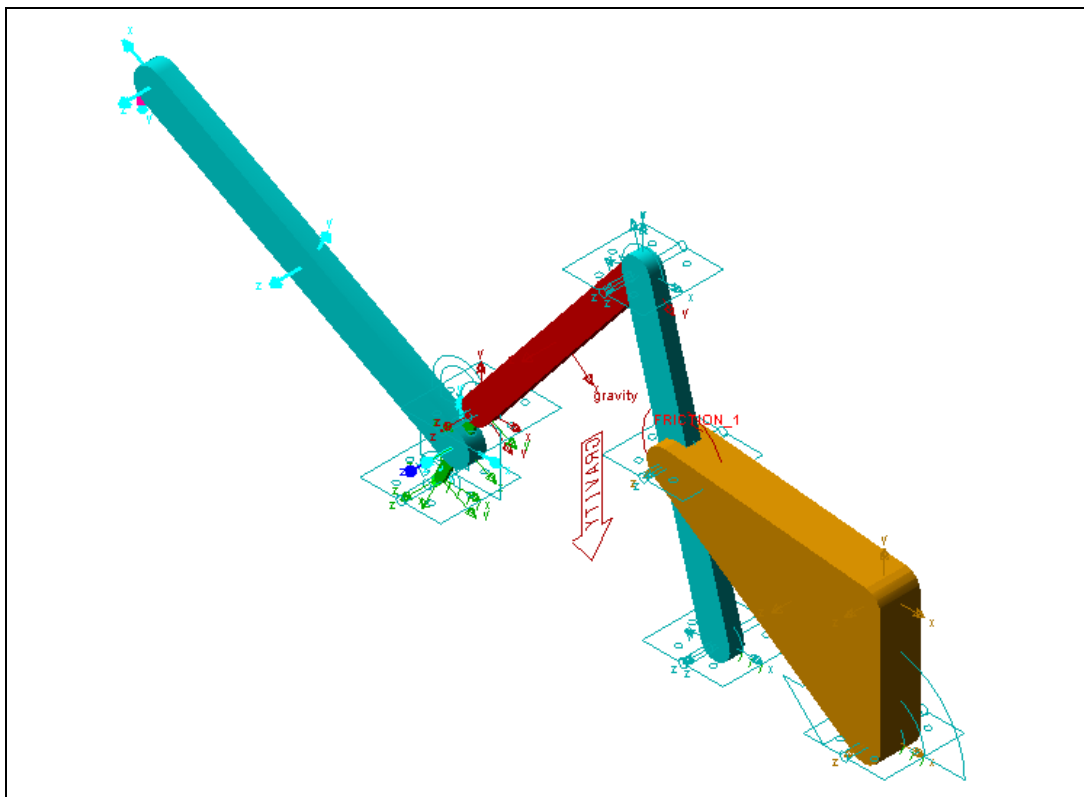
Figure 17: 2D MFI thorax simulation set-up (Design 1)

DESIGN 2

Figure 18: 2D MFI thorax simulation set-up (Design 2)

CHAPTER 5
CONCLUSION AND RECOMMENDATION

In this project, there are certain areas that can be improved in the future. Improvement needed to optimize the performance of the MFI as well as to gain the best output out of it. Research has been done and ultimately, the problems were identified and the task is to come out with the best solution.

5.1 Material Selection for MFI

Material selection for MFI fabrication is important since minimizing the weight of the MFI is the main target for the MFI to be able to lift up in the air. Selection of material with high stiffness, light weight, and easy to fabricate is the main target before proceeding with the micro fabrication of MFI. The body of the MFI (Air frame), which acquire most of the robot's weight is best to be designed on a material which have high stiffness-to-weight properties composite material. For this purpose, polyurethane will be used for the air frame. Polyurethane formulations cover an extremely wide range of stiffness, hardness, and densities.

For thorax (four bar linkages) construction, hollow beams of M60J UHM carbon fiber reinforced epoxy is recommended since it has high stiffness-to-weight ratio. The final 1 degree of freedom thorax is the connection between links. For this purpose, polyester flexure can be used as joints by stacking it between 2 layers carbon fiber (links).

5.2 Micro fabrication of MFI

Fabrication of MFI is essential for this project completion. Electrical Discharge Machining (EDM) is proposed for this purpose, since it has the ability to cut pieces with high dimension accuracy. EDM is able to produce cuttings up to ±0.1mm of resolution. EDM is the process of electrically removing material from any conductive work piece by applying high-frequency pulsed, AC, or DC current to the work piece through an electrode or wire, which melts and vaporizes the work piece material. This process is used when the work piece material is too hard, or the shape or location of the detail cannot easily be conventionally machined. The electrode never touches the work piece but discharges its potential current through an insulating dielectric fluid (water or oil) across a very small spark gap.

Anticipation of EDM for the fabrication process is due to these advantages:

- No cutting force generated
- Superior surface finish
- Intricate details
- Accuracy/Repeatability
- Well suited for automation
- Allows heat treatment before EDM process, eliminating the risk of distortions.

5.3 Piezoelectric Actuator

The basic actuator is obtained by bonding together elastic layer and PZT respectively. The stiffness actuator is designed to resonate with the wing inertia reflected through an amplifying four-bar mechanism. A rigid extension can be attached to the actuator and acting as a lever, which provides larger free displacement at the tip.
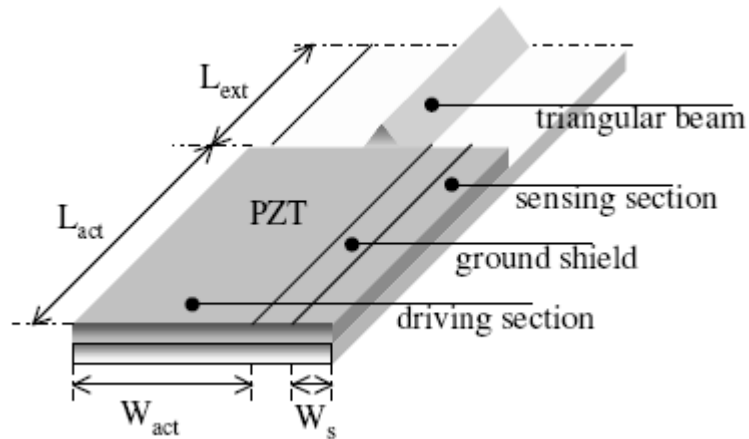
Figure 19: Piezoelectric actuator with a rigid extension (Source from Development of Piezoelectric Sensors for Micromechanical Flapping Mechanisms)

A hollow triangular beam can be bonded on top of the extended actuator. Such a folded structure is much stiffer than a planar structure. It can be made out of thinner, lighter, stainless steel and still be considered rigid.

5.4 Project Conclusion

For the conclusion, the methodology on this project can be used to support the objective which is to design a micromechanical flying insect model and possible mechanism for the flapping of wings of fly robot actuated by piezoelectric. At the research and design stage, it does give me a better view on the product that is going to be fabricated and hence develop my personal skills and knowledge in the mechanical design field.

REFERENCES

Journals / Literature

1. Microrobotics Using Composite Materials: The Micromechanical Flying Insect Thorax*. Department of EECS, University of California, 2003.

2. S. Avadhanula, R. J. Wood, D. Campolo, and R. S. Fearing. Dynamically tuned design of the MFI thorax. In Proc. of ICRA, 2002.

3. X. Deng, L. Schenato, and S.S. Sastry. Hovering flight control of a micromechanical flying insect. In Proc. Of the 40th CDC, 2001.

4. Neurotechnology for Biometic Robots, Editors: Joseph Ayers, Joel L Davis & Alan Rudolph (MIT Press) 2002

5. Proceedings of the 2003 IEEE International Conference on Robotics & Automation: Microrobotics Using Composite Materials

Websites (with date of access)

1. http://robotics.eecs.berkeley.edu/~ronf/mfi.html (September 2007)

2. http://www.cis.plym.ac.uk/cis/InsectRobotics/Technology.htm (September 2007)

3. http://robotics.eecs.berkeley.edu/%7Eronf/MFI/thorax.html (September 2007)

4. http://www.kentleech.com/index.html (January 2008)

5. http://robotics.eecs.berkeley.edu/ronf/mfi.html (September 2007)

6. http://www.piezo.com/index.html (February 2008)

7. http://science.howstuffworks.com/spy-fly.htm (September 2007)

8. http://robotics.eecs.berkeley.edu/%7Eronf/Biomimetics.html (September 2007)